

ULRR

Colloidal synthesis of wurtzite Cu₂ZnSnS₄ nanorods and their perpendicular assembly

Item Type	Article
Authors	Singh, Ajay;Geaney, Hugh;Laffir, Fathima R.;Ryan, Kevin M.
Citation	Journal of the American Chemical Society;134(6), pp. 2910-2913
Publisher	American Chemical Society
Download date	2026-03-13 19:49:34
Item License	https://creativecommons.org/licenses/by-nc-sa/1.0/
Link to Item	https://hdl.handle.net/10344/2986

Colloidal Synthesis of Wurtzite $\text{Cu}_2\text{ZnSnS}_4$ Nanorods and Their Perpendicular Assembly

Ajay Singh,^{1,2} Hugh Geaney,¹ Fathima Laffir¹ and Kevin M Ryan^{*1,2}

¹ Materials and Surface Science Institute (MSSI), Department of Chemical and Environmental Sciences, University of Limerick, Limerick, Ireland.

²The SFI-Strategic Research Cluster in Solar Energy Research.

CZTS, Nanorod, Nanocrystal, Copper Zinc Tin Tetrasulphide, Copper Chalcogenide, Nanorod Assembly

Supporting Information Placeholder

ABSTRACT: The quaternary copper chalcogenide, $\text{Cu}_2\text{ZnSnS}_4$, is an important emerging material for the development of low cost and sustainable solar cells. Here we report a facile solution synthesis of stoichiometric $\text{Cu}_2\text{ZnSnS}_4$ in size controlled nanorod form (11 × 35 nm). The monodisperse nanorods have a band gap of 1.43 eV and can be assembled into perpendicularly aligned arrays by controlled evaporation from solution.

Colloidal semiconductor nanocrystals are a remarkable material set, that can be synthesized and processed as a ‘chemical’ in high yield while exhibiting optical and electronic properties that are size dependent.¹ Applications ranging from bio-labeling to photocatalysis and photovoltaics have emerged exploiting either the discrete or collective properties of these size controlled crystals.² The synthesis of the archetypal binary (II-VI) nanocrystals has progressed to the point where precise control over their size, shape, composition and crystal phase is routine thereby rapidly accelerating the advances that utilize these as building blocks.^{1b,3} Extension of colloidal nanocrystal synthesis to ternary and quaternary semiconductors has the capacity to greatly expand this research platform.^{4,5}

In particular, copper based ternary and quaternary semiconductors such as $\text{CuInS}(\text{Se})_2$ (CIS), $\text{CuIn}_x\text{Ga}_{1-x}\text{S}(\text{Se})_2$ (CIGS) and $\text{Cu}_2\text{ZnSnS}(\text{Se})_4$ (CZTS) are of interest due to their high absorption coefficients, low toxicity and suitable band gap for solar energy conversion.^{4,6} Advances in the colloidal synthesis and shape control of nanocrystal CIS and CIGS have been demonstrated although similar reports with CZTS remain elusive.^{4c,4e} CZTS is flagged as the material most likely to allow unrestricted PV application on a global scale, given the relatively abundant nature of Zn and Sn in comparison to In and Ga and the promising efficiencies of 9.7%.^{6,7} Generating CZTS in nanocrystal form allows absorber layer production by simple solution processes (spin-casting, spraying or printing methods) dramatically offsetting the cost of expensive vacuum processes.^{6b,7,8b} While synthesis of 0D CZTS nanocrystals in the tetragonal crystal structure,^{5a-5c} has been achieved, their formation in the more attractive rod geometry remains elusive. In nanorods, maximization of total absorption and directional charge transfer is possible by controlling the length while retaining the diameter dependent properties such as band gap. Moreover, control of

orientation and positioning such that each nanorod is vertically aligned and close packed allows their collective properties to be harnessed at a device scale.^{9,11}

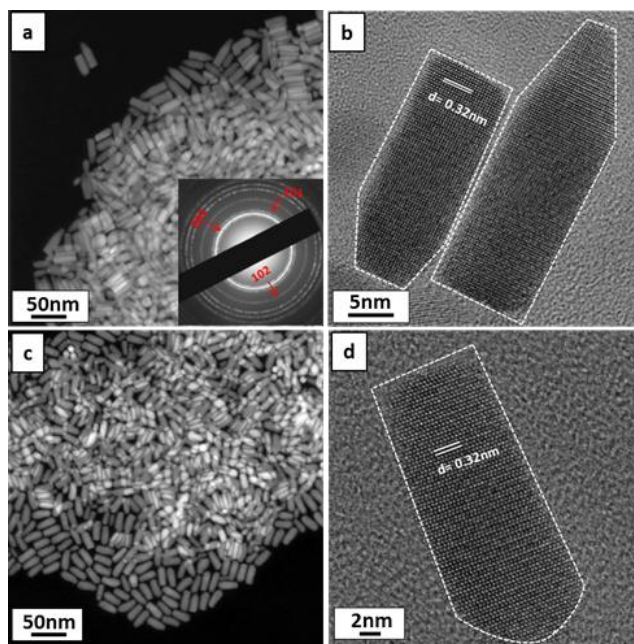


Figure 1. (a) Dark-field STEM (DF-STEM) image of bullet shaped CZTS nanorods with inset showing the corresponding Selected Area Diffraction Pattern (SAED). (b) HRTEM image showing the bullet shaped CZTS nanorods are elongated in [002] direction. (c) DF-STEM image of CZTS nanorods synthesized in the presence of a higher 1-DDT concentration. (d) HRTEM image of single CZTS nanorod.

Herein we describe a colloidal synthesis of monodisperse stoichiometric $\text{Cu}_2\text{ZnSnS}_4$ nanorods in high yield. The quaternary semiconductor nanorods occur in the wurtzite crystal structure with elongation occurring along the [002] direction and exhibit a band gap of 1.43 eV. This crystal phase is attractive not just for shape control but is also known to allow wide range tuning of the band gap due to random distribution of In/Sn and Ga/Zn ions in the crystal structure.^{4f,4g,5f} We further demonstrate the subsequent assembly of the rods into superstructures with each rod close packed and orientated orthogonal to the substrate. The rod geometry, hierarchical assembly

and optimal crystal structure makes this route of significant interest for low cost PV devices.

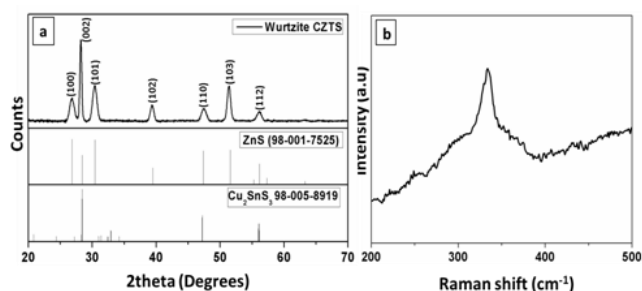


Figure 2. (a) XRD pattern of as-synthesized wurtzite CZTS nanorods. For reference, the XRD pattern of wurtzite ZnS (PCPDF no. 98-001-7525) and monoclinic Cu_2SnS_3 (PCPDF no. 98-005-8919) are also shown. (b) Raman spectra of CZTS nanorods.

In a typical synthesis, copper(II) acetylacetonate (0.261g, 1mmol), Zinc acetate (0.091g, 0.5mmol), Tin(IV) acetate (0.177g, 0.5mmol) and TOPO (1.353g, 3.5mmol) were mixed with 10mL of 1-octadecene in a three-neck round-bottom flask and evacuated at room temperature for 30-45mins. The solution was then heated to 240-260°C under an argon atmosphere. At 150- 160°C, a mixture of 0.25mL 1-DDT and 1.75mL t-DDT was quickly injected into the flask which resulted in an immediate color change from dark green to wine red and then finally to brown. After injection, the reaction was allowed to proceed for 15-30 minutes with continuous stirring. Nanorod growth was terminated by removal of the heating mantle and at 80°C, 2-4 ml anhydrous toluene were added to the mixture to quench the reaction. The nanorods were then washed in a 1:1 ratio of toluene to ethanol and centrifuged at 4000rpm for 10mins to yield a brownish centrifuged product.

The dark-field STEM (DF-STEM) image in figure 1a shows that the nanorods formed show good monodispersity with average lengths of $35 \pm 3\text{nm}$ and diameters of $11 \pm 0.5\text{nm}$. The as-synthesized CZTS nanorods are predominantly bullet shaped with ~7% polydispersity that can be improved by size-selective precipitation. The polycrystalline electron diffraction pattern shown in inset figure 1a is indexed with rings to (002), (101) and (102), which correspond to the wurtzite phase of CZTS. High-resolution TEM (HRTEM) images of an individual bullet shaped nanorod (figure 1b) showed lattice fringes with spacing of $d = 0.32$ which corresponds to the (002) lattice plane of the wurtzite CZTS structure. This growth direction along the c-axis is characteristic of the wurtzite phase^{3a,3c,4c-4e} and its preferred formation in this synthesis, rather than kesterite, is critical to elongation. The key for stabilizing the wurtzite phase rather than kesterite is the use of dodecanethiol in the reaction as it acts both as a sulfur source and ligand. Dodecanethiol has been previously reported as a strong coordinating ligand for the wurtzite copper-based chalcogenide nanocrystals, CIS and CIGS.^{4c-4e,5f} While studying the effect of thiols (1-DDT and t-DDT) on the formation of wurtzite CZTS nanocrystals we observed that a combination of both is necessary for the nanorods to form. In addition, single phase CZTS nanorods were formed only when the thiols were injected at temperature $<200^\circ\text{C}$ to avoid the formation of unwanted Cu_2S side products. Synthesis carried out in the presence of only 1-DDT (see detail in Supporting information) yields only smaller pseudo-spherical wurtz-

ite CZTS nanocrystal (Figure S1). Conversely, if the concentration of 1-DDT is doubled in the reaction mixture, the shape of CZTS nanocrystal changes from bullet to more conventional rod shaped as seen in figure 1c. This suggests 1-DDT binds more strongly to facets other than the (002) allowing anisotropic growth in this direction. The HRTEM image of individual rod shape CZTS nanorod shows clear lattice fringes with spacing of $d = 0.32$ nm, corresponding to (002) lattice planes of the wurtzite structure.

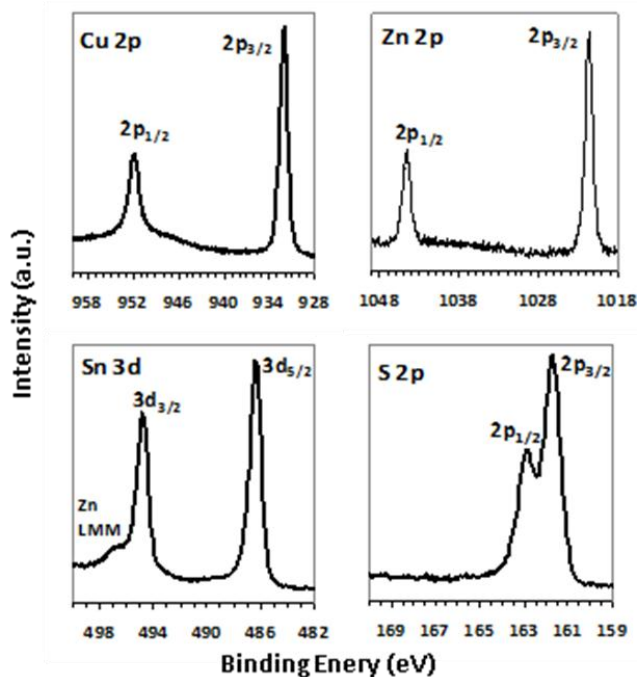


Figure 3. High-resolution XPS analysis of CZTS nanorods.

XRD was investigated as a bulk analysis technique to ensure compositional homogeneity across the nanorod samples. A resultant XRD diffractogram can be seen in figure 2a with major reflections at 2theta values which correspond to (100), (002), (101), (102), (110), (103) and (112) planes of hexagonal structure and match well with the previously reported CZTS wurtzite structure.^{5f} This structure can be derived from wurtzite ZnS by substitution of Zn with Cu and Sn atoms.^{5f} In particular, the XRD pattern of wurtzite CZTS matches the combined reflections from hexagonal ZnS and monoclinic Cu_2SnS_3 , as seen in figure 2a. The single Raman peak at 333cm^{-1} is close to the value reported for bulk CZTS (figure 2b).¹² The noted broadening of the Raman peak has been shown before for nanocrystals and is due to the phonon confinement within the nanocrystal.¹³ It is noticeable that there are no additional peaks for other phases such as ZnS, SnS and Cu_2S which confirms the single phase of CZTS nanorods.

X-ray photoelectron spectroscopy was performed to investigate the chemistry of the CZTS nanorods. Survey spectrum of the synthesized nanorods identifies the presence of the Cu, Zn, Sn, S, O and C (Figure S2). High resolution spectra of Zn 2p, Cu 2p, Sn 3d and S 2p were measured to determine the oxidation states of the constituent elements (figure 3). The narrow doublet peaks of Cu 2p spectrum (figure 3) appear as a doublet with $2p_{3/2}$ at 932.1 eV and $2p_{1/2}$ at 951.9 eV with peak separation of 19.8 eV indicative of Cu (I).^{14, 4b} The peaks of Zn 2p

appear at binding energies 1021.6 eV and 1044.7 eV which can be assigned to Zn (II) with peak splitting of 23.1 eV.^{4a} The Sn (IV) state is confirmed by peaks located at 486.4 eV and 494.8 eV with its characteristic peak separation of 8.4 eV.^{14,15} The sulphur spectrum can be assigned to the presence of sulphides at binding energies 161.7 eV and 162.9 eV and doublet separation of 1.2 eV.^{14,15} Also In order to investigate the quantitative analysis of all four elements in the nanorods, Energy dispersive X-ray (EDS) equipped with an SEM was used to find the stoichiometric ratio of Cu:Zn:Sn:S is close to 2:1:1:4 (Figure S3) which corresponds well with the elemental ratio of CZTS.

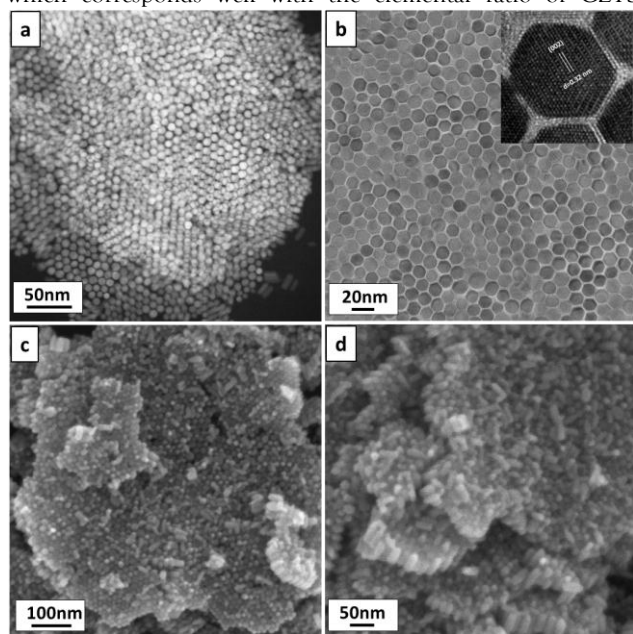


Figure 4. (a) DF-STEM image shows 3D superstructure of CZTS nanorods. (b) Top-down HRTEM images show the closed-packed monolayer of CZTS nanorods with inset HRTEM image of single rod. (c) & (d) SEM and HRSEM images show the top-down and side view of multilayer assembly of CZTS nanorods.

The as-synthesized CZTS nanorods have high uniformity across the length and diameter, which is a prerequisite for self-assembly. We have recently shown with wurtzite (II-VI) nanorods that the simplest method to achieve perpendicular assembly is to create conditions such that rods pre-organize in solution. At an optimal concentration, the inter-nanorod distance in solution is sufficient to allow attractive interparticle interaction such as dipole-dipole to overcome coulombic repulsion to allow nucleation and growth of 2D assembled sheets.^{10c,10d} The CZTS rods have a charge of 5 ± 2 mV and a permanent dipole along the [002] direction. Therefore, simply modulating the nanorod concentration over a range allows isolation of the critical concentration for preferential assembly. The top down DF-STEM image in figure 4a shows a 3D superstructure of CZTS nanorods. Figure 4b shows TEM images of a monolayer of vertically oriented CZTS nanorods where the perfect close packed hexagonal ordering can be seen. The inset top-down HRTEM image of single nanorods shows the d-spacing in the lattice fringes is 0.32 nm, which matches with the (002) plane of wurtzite structure of CZTS nanorods.

When the rate of evaporation of solvent is controlled, the 2D sheets can be deposited sequentially forming 3D multilayer

arrays as shown in figure 4c,d. Assemblies up to micron sized areas are also obtained by this approach (Supporting Information: figure S4). The band gap of CZTS nanorods was calculated using UV-vis spectra, (Supporting Information: Figure S5) at 1.43 eV by extrapolating the linear region of a plot of $(\alpha h\nu)^2$ versus energy, where α represent the absorption coefficient and $h\nu$ is photon energy.^{5f}

In conclusion, a reproducible solution synthesis has been reported to synthesize high quality monodisperse wurtzite $\text{Cu}_2\text{ZnSnS}_4$ nanorods. The rods are defect free single crystals with a band-gap in the visible part of the electromagnetic spectrum. The constituent elements of these rods, are non-toxic and in high abundance allowing for a wide range of low cost applications exploiting their absorption or emission properties e.g. biolabels, fluorescent emitters or photocatalysis. Their facile organization into close packed and vertically oriented arrays on the substrate strengthens their potential for use as solar absorber layers where directional orientation and length control will likely allow for enhanced efficiencies^{9b,16}

ASSOCIATED CONTENT

(Detailed experimental procedure. TEM images of pseudo-spherical wurtzite CZTS nanocrystal and XRD pattern, EDX and XPS survey spectra, Additional SEM images. This material is available free of charge via the Internet at <http://pubs.acs.org>.

Corresponding Author

Kevin.m.ryan@ul.ie

ACKNOWLEDGMENT

This work was supported by Science Foundation Ireland (SFI) through the Principal Investigator program; Contract No. 06/IN.1/185 and the Solar Energy Conversion Strategic Research Cluster [07/SRC/B1160]. This work was also conducted under the framework of the INSPIRE project, funded by the Irish Government's Program for Research in Third Level Institutions, Cycle 4, National Development Plan 2007-2013.

REFERENCES

- (1) (a) Alivisatos, A. P. *Science* **1996**, 271, 933. (b) Talapin, D. V.; Lee, J. S.; Kovalenko, M. V.; Shevchenko, E. V. *Chem. Rev.* **2010**, 110, 389.
- (2) (a) Bruchez, M.; Moronne, M.; Gin, P.; Weiss, S.; Alivisatos, A. P. *Science* **1998**, 281, 1203. (b) Sanyal, A.; Bala, T.; Ahmed, S.; Singh, A.; Piterina, A. V.; McGloughlin, T. M.; Laffir, F. R.; Ryan, K. M. *J. Mater. Chem.* **2009**, 19, 8974. (c) Chen, X.; Shen, S.; Guo, L.; Mao, S. S. *Chem. Rev.* **2010**, 110, 650. (d) Gur, I.; Fromer, N. A.; Geier, M. L.; Alivisatos, A. P. *Science* **2005**, 310, 46.
- (3) (a) Peng, X. G.; Manna, L.; Yang, W. D.; Wickham, J.; Scher, E.; Kadavanich, A.; Alivisatos, A. P., *Nature* **2000**, 404, 59. (b) Regulacio, M.; Han, M. *Acc. Chem. Res.* **2010**, 43, 621. (c) Yin, Y.; Alivisatos, A. P., *Nature* **2005**, 437, 664.
- (4) (a) Guo, Q.; Kim, S. J.; Kar, M.; Shafarman, W. N.; Birkmire, R. W.; Stach, E. A.; Agrawal, R.; Hillhouse, H. W. *Nano Lett.* **2008**, 8, 2982. (b) Norako, M. E.; Franzman, M. A.; Brutchey, R. L. *Chem. Mater.* **2009**, 21, 4299. (c) Kruszynska, M.; Borchert, H.; Parisi, J.; Kolny-Olesiak, J. J. *Am. Chem. Soc.* **2010**, 132, 15976. (d) Wang, Y.-H. A., Zhang, X., Bao, N., Lin, B., Gupta, A. *J. Am. Chem. Soc.* **2011**, 133, 11072. (e) Lu X, Zhuang Z, Peng Q, Li Y., *CrystEngComm*, **2011**, 13, 4039. (f)

- Qi, Y., Liu, Q., Tang, K., Liang, Z., Ren, Z., and Liu, X. *J. Phys. Chem. C* **2009**, 113, 3939. (g) Pan, D.; An, L.; Sun, Z.; Hou, W.; Yang, Y.; Yang, Z.; Lu, Y. *J. Am. Chem. Soc.* **2008**, 130, 5620. (h) Connor, S. T.; Hsu, C.-M.; Weil, B. D.; Aloni, S.; Cui, Y. *J. Am. Chem. Soc.* **2009**, 131, 4962. (i) Koo, B.; Patel, R. N.; Korgel, B. A. *J. Am. Chem. Soc.* **2009**, 131, 3134. (j) Norako, M. E.; Brutchey, R. L. *Chem. Mater.* **2010**, 22, 1613. (k) Steinhagen, C.; Akhavan, V. A.; Goodfellow, B. W.; Panthani, M. G.; Harris, J. T.; Holmberg, V. C.; Korgel, B. A. *ACS Appl. Mater. Interfaces* **2011**, 3, 1781.
- (5) (a) Riha, S. C.; Parkinson, B. A.; Prieto, A. L. *J. Am. Chem. Soc.* **2009**, 131, 12054. (b) Zou, C.; Zhang, L. J.; Lin, D. S.; Yang, Y.; Li, Q.; Xu, X. J.; Chen, X. A.; Huang, S. M. *CrystEngComm* **2011**, 13, 3310. (c) Guo, Q.; Ford, G. M.; Yang, W.-C.; Walker, B. C.; Stach, E. A.; Hillhouse, H. W.; Agrawal, R. *J. Am. Chem. Soc.* **2010**, 132, 17384. (d) Riha, S. C.; Parkinson, B. A.; Prieto, A. L. *J. Am. Chem. Soc.*, **2011**, 133, 15272. (e) Larsen, T. H.; Sigman, M.; Ghezellash, A.; Doty, R. C.; Korgel, B. A. *J. Am. Chem. Soc.* **2003**, 125, 5638. (f) Lu, X.; Zhuang, Z.; Peng, Q.; Li, Y. *Chem. Commun.* **2011**, 47, 3141. (g) Shavel, A.; Arbiol, J.; Cabot, A. *J. Am. Chem. Soc.* **2010**, 132, 4514. (h) Norako, M. E.; Greaney, M. J.; Brutchey, R. L. *J. Am. Chem. Soc.*, **2012**, 134, 23. (i) Deka, S.; Genovese, A.; Zhang, Y.; Miszta, K.; Bertoni, G.; Krahne, R.; Giannini, C.; Manna, L. *J. Am. Chem. Soc.* **2010**, 132, 8912. (j) Zhuang, Z. B.; Peng, Q.; Zhang, B.; Li, Y. D. *J. Am. Chem. Soc.* **2008**, 130, 10482. (k) Wang, J.-J.; Wang, Y.-Q.; Cao, F.-F.; Guo, Y.-G.; Wan, L.-J. *J. Am. Chem. Soc.* **2010**, 132, 12218.
- (6) (a) Wadia, C., Alivisatos, A. P., and Kammen, D. M. *Environ. Sci. Technol.* **2009**, 43, 2072. (b) Habas, S. E.; Platt, H. A. S.; van Hest, M. F. A. M.; Ginley, D.S. *Chem. Rev.* **2010**, 110, 6571. (c) van Hest, M. F. A. M. and Ginley, D. S. (2008) Future Directions for Solution-Based Processing of Inorganic Materials, in *Solution Processing of Inorganic Materials* (ed D. B. Mitzi), John Wiley & Sons, Inc., Hoboken, NJ, USA. doi: 10.1002/9780470407790.ch14
- (7) Todorov, T. K., Reuter, K. B., and Mitzi, D. B. *Adv. Mater.* **2010**, 22 E156.
- (8) (a) Sargent, E. H. *Nat. Photonics* **2009**, 3, 325. (b) Guo, Q., Hillhouse, H. W., and Agrawal, R. *J. Am. Chem. Soc.* **2009**, 131, 11672.
- (9) (a) Hu, J. T.; Li, L. S.; Yang, W. D.; Manna, L.; Wang, L. W.; Alivisatos, A. P., *Science* **2001**, 292, 2060. (b) Krahne, R.; Morrello, G.; Figuerola, A.; George, C.; Manna, L. *Phys. Rep.* **2011**, 501, 75. (c) Gonzalez-Valls, I.; Lira-Cantu, M. *Energy Environ. Sci.* **2009**, 2, 19.
- (10) (a) Ahmed, S.; Ryan, K. M. *Chem. Commun.* **2009**, 6421. (b) Ryan, K. M., Mastroianni, A., Stancil, K. A., Liu, H. T., Alivisatos, A. P. *Nano Lett.*, **2006** 6, 1479. (c) Singh, A.; Gunning, R. D.; Sanyal, A.; Ryan, K. M. *Chem. Commun.*, **2010** 46, 7193. (d) Singh, A.; Gunning, R. D.; Ahmed, S.; Barrett, C. A., English, N. J.; Garate, José-Antonio; Ryan, K. *J. Mater. Chem.*, **2012**, 22, 1562. (e) M. Zanella, M.; Gomes, R.; Povia, M.; Giannini, C.; Zhang, Y.; Riskin, A.; van Bael, M.; Hens, Z.; Manna, L. *Adv. Mater.* **2011**, 23, 2205.
- (11) (a) Baker, J. L.; Widmer-Cooper, A.; Toney, M. F.; Geissler, P. L.; Alivisatos, A. P. *Nano Lett.* **2010**, 10, 195. (b) Ahmed, S.; Ryan, K. M. *Nano Lett.* **2007**, 7, 2480. (c) Baranov, D. et al. *Nano Lett.* **2010**, 10, 743. (d) Kelly, D.; Singh, A.; Barrett, C. A.; O'Sullivan, C.; Coughlan, C.; Laffir, F. R.; O'Dwyer, C.; Ryan, K. M., *Nanoscale* **2011**, 3, 4580.
- (12) Fernandes, P. A., Salome, P. M. P., and da Cunha, A. F. *Thin Solid Films* **2009**, 517, 2519.
- (13) Bersani, D.; Lottici, P. P.; Ding, X. *Appl. Phys. Lett.* **1998**, 72, 73.
- (14) NIST-XPS database, version 3.5 (<http://srdata.nist.gov/xps/>).
- (15) Moulder, J. F.; Stickle, W. F.; Sobol, P. E.; Bomben, K. D. *Handbook of X-Ray Photoelectron Spectroscopy*, Perkin-Elmer, Corporation Physical Electronics Division, 1992.
- (16) (a) Kriegel, I.; Rodriguez-Fernandez, J.; Como, E. D.; Lutich, A. A.; Szeifert, J. M.; Feldmann, J. *Chem. Mater.* **2011**, 23, 1830. (b) Hore, M. J. A.; Composto, R. J. *ACS nano* **2010**, 4, 6941 (c) Kriegel, I.; Jiang, C., Rodriguez-Fernandez, J.; Schaller, R. D.; Talapin, D V.; Da Como, E.; Feldmann, J. *J. Am. Chem. Soc.*, **2012**, DOI: 10.1021/ja207798q. (d) Li, W.; Döblinger, M.; Vaneski, A.; Rogach, A. L.; Jäckel F.; Feldmann J. *J. Mater. Chem.*, **2011**, 21, 17946. (e) Wang, J. J.; Xue, D. J.; Guo, Y.G.; Hu, J. S.; Wan, L. J; *J. Am. Chem. Soc.*, **2011**, 133, 18558.

Insert Table of Contents artwork here

